

Data-driven approach in a compartmental epidemic model to assess undocumented infections

Guilherme S. Costa ¹, Wesley Cota ¹, and Silvio C. Ferreira ^{1, 2}

¹*Departamento de Física, Universidade Federal de Viçosa, 36570-900 Viçosa, Minas Gerais, Brazil*

²*National Institute of Science and Technology for Complex Systems, 22290-180, Rio de Janeiro, Brazil*

Nowcasting and forecasting of epidemic spreading rely on incidence series of reported cases to derive the fundamental epidemiological parameters for a given pathogen. Two relevant drawbacks for predictions are the unknown fractions of undocumented cases and levels of nonpharmacological interventions, which span highly heterogeneously across different places and times. We describe a simple data-driven approach using a compartmental model including asymptomatic and pre-symptomatic contagions that allows to estimate both the level of undocumented infections and the value of effective reproductive number R_t from time series of reported cases, deaths, and epidemiological parameters. The method was applied to epidemic series for COVID-19 across different municipalities in Brazil allowing to estimate the heterogeneity level of under-reporting across different places. The reproductive number derived within the current framework is little sensitive to both diagnosis and infection rates during the asymptomatic states. The methods described here can be extended to more general cases if data is available and adapted to other epidemiological approaches and surveillance data.

I. INTRODUCTION

Our contemporary society is facing an unprecedented threat imposed by the COVID-19, caused by the pathogen SARS-CoV-2, evidencing the importance, limitations, and subtleties of using compartmental epidemic models for the forecasting or nowcasting of pandemic scenarios [1–5]. After two years of intensive investigation, much has been learned with respect to the virology of SARS-CoV-2 in humans [6–9]. Among other achievements, several key aspects of the transmission were unveiled [5, 10–12] and efficient vaccines have been developed [13]. Variants of the original strain [14, 15] give rise to new and more aggressive outbreaks due to reinfection and raised contagion rates that tend to become endemic, circulating among humans indefinitely with new outbreaks emerging seasonally [16]. Whilst the biology of the virus and interaction with human hosts is better understood, other crucial aspects of the epidemiology, specially the behavioral ones, remains unpredictable even at a short-term, varying across time and location. In particular, the non-pharmaceutical interventions (NPIs), such as face masks, testing policies and social distancing have played a central role on the spreading of SARS-CoV-2 [17–20]. The aforementioned NPIs contribute for reduction of the contagion rates in an uncontrolled way, such that the effective contagion rate must be inferred along the time from count case series via likelihood or other calibration methods [21, 22].

A fundamental epidemic characteristic of the SARS-CoV-2 contagion in humans is its high transmission before the onset of the symptoms [5, 11, 23], the presymptomatic individuals, and even the contagion by those who never manifest relevant symptoms [24, 25], the true asymptomatic individuals. The latter could be accessed by mass testing and contact tracing, for example. Seroprevalence studies for different phases and regions [14, 26] reveal population incidences of antibodies for SARS-

CoV-2 in levels much higher than the case counts reported by the epidemiological surveillance systems. So, the case fatality ratio (CFR), defined as the ratio between the numbers of diagnosed deaths and cases, can differ substantially from the infection fatality ratio (IFR), defined as the fraction of all infections (documented or not) that evolve to death [26, 27].

The level of under-reporting, in which the CFR is greater than the IFR, varies widely in different seroprevalence inquiries [26] due to several uncontrolled factors such as the testing policies (only symptomatic cases, contact tracing, etc.), availability of tests (low or high income places), sensitivity of tests (antigen or PCR), and seeking for medical care, among others. The relation between seropositivity and immunity is not fully established and new emerging variants always open paths for reinfections and new outbreaks [28]. Therefore, to estimate the level of undocumented infections across different places and times remains a challenge. Epidemic models of statistical inference were developed to access the amount of undocumented infections of SARS-CoV-2. For example, Pullano et al. [29] estimated that 9 out 10 cases of symptomatic infections were not ascertained by the surveillance system in France from 11 May to 28 June 2020, during the first epidemic wave of COVID-19, suggesting that large numbers of symptomatic cases of COVID-19 did not seek for medical advice. Lu et al. [30] considered four complementary approaches to estimate the cumulative incidence of symptomatic cases of COVID-19 in the US and concluded that on April 4 of 2020 the estimated case count was 5 to 50 times higher than the official counts of positive tests across the different states. Subramanian et al. [31] used a model including testing information to fit the case and serology data from New York City, from March to June of 2020, to estimate a low proportion of symptomatic cases (13 to 18% of the total infections), and that the reproductive number could be larger than often assumed. Similarly, Irons

and Raftery [32] used a similar approach to estimate that approximately 60% of the infections were not diagnosed by tests in USA as of March 7, 2021. Hallal et al. [33] carried out two seroprevalence studies, the first in May 2020 and the second in June 2020, in 133 municipalities of Brazil and estimated that only 10.3% of all infections were documented.

Due to the importance of asymptomatic or pre-symptomatic transmission, the corresponding compartments were soon included in mathematical models for COVID-19 [11, 34–37]. However, it is concomitantly an additional source of uncertainty in the initial conditions. Predictive scenarios of the first SARS-CoV-2 outbreak were either semi-quantitative [34, 38, 39] or based on Bayesian inference using reported cases’ series [35, 40, 41]. Brazil is an example, certainly not an exception, of highly heterogeneous responses to COVID-19 pandemics due to the lack of coordinated policies across different administrative layers [42], in addition to the intrinsic variability of social-economic indexes across the country impacting directly the epidemiological outcomes. Therefore, a mechanistic approach for simulation of epidemic spreading with asymptomatic transmission calls for a systematic way to determine the initial conditions.

The contribution of asymptomatic infections and testing policies to the effective reproductive number R_t [43] through surveillance counts is an important issue [31, 32]. The basic reproductive number is defined as the average number of secondary infections generated by a single infected individual introduced in a completely susceptible population, commonly represented by R_0 . The effective reproductive number is given by $R_t = S(t)R_0$, where $S(t)$ is the fraction of susceptible population (who can be infected by the pathogen) at time t . This definition, under the hypothesis of homogeneous mixing, is the simplest one and can be generalized to stratified compartments [43]. The reproductive number can also be estimated directly from case counts using statistical inference models [21], as reported for COVID-19 pandemics across the world [18, 35, 42, 44].

In this present work, we describe a mechanistic approach to estimate the number of undocumented infections (symptomatic or not) using the epidemic surveillance data for confirmed cases and deaths. The method is grounded on a compartmental epidemic model including both documented and undocumented compartments, the latter not counted by epidemiological surveillance. The present approach allows to determine the effective reproductive number, the level of under-reporting and initial conditions using the date of diagnosis. The approach can be promptly modified or generalized for other types of data, epidemic compartments, and population stratification. The method shares similarities with the recent approaches to estimate undocumented cases [24, 29, 30, 32], such as the use of reported infections and deaths. The central difference is that our approach is essentially mechanistic and not Bayesian.

We applied the method across different geographi-

cal scales of two Brazilian states, namely Paraná (PR) and Espírito Santo (ES), using time series with dates of COVID-19 diagnosis available by the epidemiological surveillance of the respective states. The time window of investigation was from 1 January to 31 July of 2021, encompassing the second epidemic wave driven mainly by the Gamma variant [42, 45]. We report variable levels of under-reporting across different places and times. We were able to estimate initial conditions for the hidden compartments and effective infection rates along the time, which gave an efficient short-time forecast for the series of confirmed cases. Despite the basic reproductive number being explicitly dependent on the asymptomatic transmission, the analysis indicates that undocumented infections seem to not alter significantly the effective reproductive number for the analyzed series.

The remaining of this paper is organized as follows. The methodology is detailed in section II. The epidemic compartmental model and some analytical results are presented in subsection II A. The data-driven approach to estimate the under-reporting level from epidemiological surveillance counts is described in subsection II B while the eigenvalue approach to determine the initial conditions is presented in subsection II C. Application of the method to epidemiological data is presented in section III and the main conclusions of the work are discussed in section IV.

II. A MECHANISTIC APPROACH TO ESTIMATE UNDOCUMENTED CASES

A. Compartmental model

Following a mechanistic approach for population fractions, an epidemic process with presymptomatic, asymptomatic, and undocumented transmissions are investigated using a compartmental model [43] under the homogeneous mixing hypothesis. Individuals are grouped according to their epidemic states in the following compartments: *Susceptible* (S) who can be infected; *exposed* (E) who were infected but is not contagious yet; *asymptomatic* (A) who are infectious but do not present symptoms; *symptomatic* (I) ones who may seek for medical care due to the presence of symptoms; *undocumented recovered* (R) who have been infected, healed but not diagnosed; *deceased* (D) who died due to COVID-19; two compartments of *diagnosed cases* for SARS-CoV-2 including individuals who were *asymptomatic* (C_A) or *symptomatic* (C_I) at the moment of testing; and the corresponding *recovered compartments for confirmed cases* R_A and R_I . We assume constant rates and spontaneous transitions implying that the time last in a given infectious compartment is exponentially distributed [43], in contrast with the Biology of infectious pathogens where one expects a peaked distribution that excludes very short and very long exiting times. However, multiple infectious compartments soften the problem producing

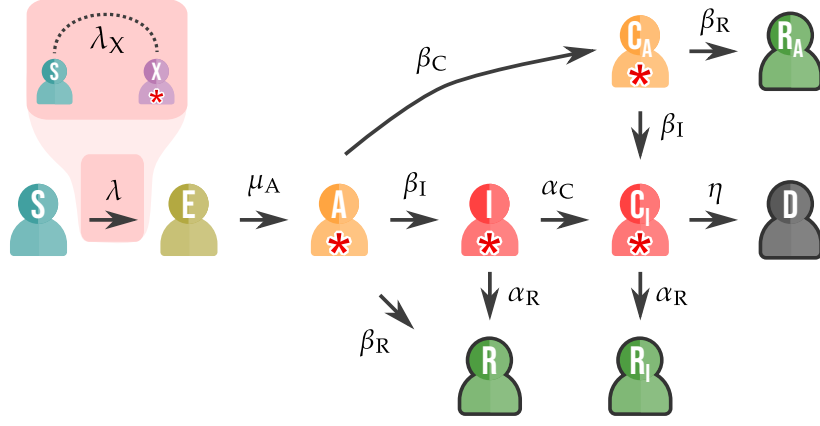


FIG. 1. Schematic representation of the epidemic model including the following compartments: susceptible (S), exposed (E), asymptomatic (A), symptomatic (I), recovered (R, R_A , and R_I), deceased (D), and confirmed cases (C_A and C_I). The transition and respective rates are indicated by arrows. The infectious compartments are depicted with the symbol \star . The infection processes, represented by the dashed line, involve the interaction between susceptible and one of the infectious compartments, happening with rates λ_X , $X=A, I, C_A$, and C_I , which may depend on the compartment.

peaked distributions for the total infectious time with a negligible probability of recovering shortly [43, 46]. The epidemiological model and rates are schematically depicted in Fig. 1.

Susceptible persons in contact with infectious individuals (asymptomatic or symptomatic) become exposed with rates λ_A and λ_I , respectively. For sake of simplicity, confirmed cases are assumed to be isolated and do not contribute for new infections. The remaining transitions are represented in Fig. 1. Exposed individuals become asymptomatic with rate μ_A . The latter can evolve to a symptomatic state with rate β_I , recover with rate β_R , or be diagnosed by tests with rate β_C moving to the confirmed compartment C_A . Similarly, the undocumented symptomatic individuals can recover with rate α_R or be diagnosed and become C_I with rate α_C . The clinical state of confirmed cases evolves as does the undocumented ones. A confirmed case (C_I) can die (D) with rate η while undocumented deaths are neglected, again, for sake of simplicity. The true asymptomatic and the presymptomatic cases are implicitly considered with transitions $A \rightarrow R$ ($C_A \rightarrow R_A$) and $A \rightarrow I$ ($A \rightarrow C_A \rightarrow C_I$), respectively. Compartments C_A and C_I are simplifications of a more complex dynamics including seeking for test, time for results, and isolation.

Assuming a constant population $N = \sum_X N_X$, where N_X is the number of individuals in the compartment X, the above transitions can be summarized in the following set of differential equations

$$\partial_t S = -(\lambda_A A + \lambda_I I)S, \quad (1a)$$

$$\partial_t E = (\lambda_A A + \lambda_I I)S - \mu_A E, \quad (1b)$$

$$\partial_t A = \mu_A E - (\beta_I + \beta_R + \beta_C)A, \quad (1c)$$

$$\partial_t I = \beta_I A - (\alpha_R + \alpha_C)I, \quad (1d)$$

$$\partial_t R = \alpha_R I + \beta_R A, \quad (1e)$$

$$\partial_t C = \beta_C A + \alpha_C I, \quad (1f)$$

$$\partial_t C_A = \beta_C A - (\beta_R + \beta_I)C_A, \quad (1g)$$

$$\partial_t C_I = \alpha_C I + \beta_I C_A - (\alpha_R + \eta)C_I, \quad (1h)$$

$$\partial_t R_A = \beta_R C_A, \quad (1i)$$

$$\partial_t R_I = \alpha_R C_I, \quad (1j)$$

$$\partial_t D = \eta C_I, \quad (1k)$$

where $X = N_X/N$, $X \in \{S, E, \dots, D\}$, is the corresponding population fraction in the compartment X.

The basic reproductive number R_0 is straightforwardly computed and given by

$$R_0 = \frac{1}{\beta_I + \beta_C + \beta_R} \left[\lambda_A + \lambda_I \frac{\beta_I}{\alpha_C + \alpha_R} \right]. \quad (2)$$

Consider a more intuitive parameterization in terms of the probabilities p_A and p_I that infected individuals are diagnosed during the asymptomatic or symptomatic phases, respectively, which can be computed from the compartmental model and are given by

$$p_A = \frac{\beta_C}{\beta_I + \beta_C + \beta_R} \quad \text{and} \quad p_I = \frac{\alpha_C}{\alpha_C + \alpha_R}. \quad (3)$$

One can also show that an exposed individual ends diagnosed with probability

$$\mathcal{P}_C = p_A + (1 - p_A)\phi p_I, \quad (4)$$

where $\phi = \beta_I/(\beta_I + \beta_R)$. The first and second terms of Eq. (4) are due to diagnosis during asymptomatic and symptomatic phases, respectively. Recovering without diagnosis happens with probability $\mathcal{P}_R = 1 - \mathcal{P}_C$. Therefore, we can determine a simple relation between the final number of documented (N_C) and undocumented (N_R) infections defining the under-reporting coefficient σ_{ur} as

$$\sigma_{ur} = \frac{N_R}{N_C} = \frac{1 - \mathcal{P}_C}{\mathcal{P}_C} = \frac{(1 - p_A)(1 - \phi p_I)}{p_A + (1 - p_A)p_I \phi}, \quad (5)$$

where

$$N_C = N_{C_A} + N_{C_I} + N_{R_A} + N_{R_I} + N_D. \quad (6)$$

We can also analytically determine the model's IFR, represented by ℓ_{IFR} , considering the probabilities that exposed individuals evolve to death passing through C_A compartment or not, which are $p_A \phi \frac{\eta}{\eta + \alpha_R}$ or $(1 - p_A) \phi p_I \frac{\eta}{\eta + \alpha_R}$, respectively. The IFR becomes

$$\ell_{IFR} = [p_A + (1 - p_A)p_I] \frac{\phi \eta}{\eta + \alpha_R}. \quad (7)$$

B. Estimating under-reporting from epidemic surveillance counts

The rates μ_A , β_I , β_R , α_R , and η are biological and can, in principle, be found in epidemiological surveys [6–9, 12, 47]. The parameters λ_A and λ_I depend on behavioral aspects such as the number of potential infectious contacts per unit of time [19, 35, 39]; prophylactic attitudes by means of NPIs [48–50]; infectiousness and prevalence of new variants [14, 42, 51]; to cite only some of the most prominent issues. Similarly, the confirmation rates β_C and α_C depend on several behavioral and socioeconomic factors being highly influenced by testing policies [39, 52, 53]. All these aspects are very heterogeneously distributed across time and different places.

We describe how testing probabilities can be estimated from surveillance count series with the aid of the compartmental model of Fig. 1. Let $\mathcal{C}(t)$ and $\mathcal{D}(t)$ represent the cumulative series of confirmed cases and deaths. The CFR computed for reported cases within a given time window $[t_{cal}, t_{cal} + \Delta\tau]$ is given by:

$$\ell_{CFR} \equiv \frac{\Delta \mathcal{D}(t_{cal})}{\Delta \mathcal{C}(t_{cal} - t_{delay})}, \quad (8)$$

in which $\Delta \mathcal{C}$ and $\Delta \mathcal{D}$ refer, respectively, to the increment in the number of cases and deaths in the interval, t_{cal} is the initial time chosen for calibration, and t_{delay} is a delay between death and positive test report. The CFR is given by the conditional probability that an infection evolves to death given that it was diagnosed. If \mathbb{D} and \mathbb{T} are events of death and diagnosis of infected individual, respectively, we have that

$$\ell_{CFR} \equiv \Pr(\mathbb{D}|\mathbb{T}) = \frac{\Pr(\mathbb{D} \cap \mathbb{T})}{\Pr(\mathbb{T})} = \frac{\Pr(\mathbb{D})}{\Pr(\mathbb{T})} = \frac{\ell_{IFR}}{\mathcal{P}_C}, \quad (9)$$

where we have used the Bayes rule for conditional probabilities, the model hypothesis that only diagnosed individuals evolve to death, and Eq. (4). Rearranging the terms, one obtains

$$\frac{\ell_{IFR}}{\ell_{CFR}} = p_A + (1 - p_A) \phi p_I. \quad (10)$$

Despite its simplicity, Eq. (10) is very handy since it relates the testing rates (or probabilities) with epidemiological parameters (ℓ_{IFR} and ϕ) and quantities (ℓ_{CFR}) which can, in principle, be obtained directly from data, Eq. (8). Therefore, if the ratio $r = p_A/p_I$ is given, the testing rates can be estimated from Eq. (4) as

$$p_I = \frac{r + \phi}{2r\phi} \left[1 - \left(1 - \frac{4r\phi\mathcal{P}_C}{(r + \phi)^2} \right)^{1/2} \right]. \quad (11)$$

Equation (11) is mathematically consistent, *i.e.* $0 \leq p_I \leq 1$, if the following conditions are satisfied

$$\begin{aligned} \mathcal{P}_C &\leq r(1 - \phi) + \phi \quad \text{for } 0 \leq r \leq \frac{\phi}{2\phi - 1}, \\ \mathcal{P}_C &\geq r(1 - \phi) + \phi \quad \text{for } r \geq \frac{\phi}{2\phi - 1}. \end{aligned} \quad (12)$$

The under-reporting coefficient, which can be expressed as

$$\sigma_{ur} = \frac{1 - \mathcal{P}_C}{\mathcal{P}_C} = \frac{\ell_{CFR}}{\ell_{IFR}} - 1, \quad (13)$$

is extracted directly from data using Eq. (8) and is used to estimate p_A and p_I for a given ratio r , which may play a role on the determination of infection rates λ_A and λ_I ; see Sec. II C.

A sensibility analysis of the ratio r can be used to verify whether the results are little sensitive to this choice (it was the case for all data analyzed in this work); otherwise the ratio must be determined using some calibration or likelihood method. Eventually, surveillance data can provide a CFR smaller than the IFR estimates which is inconsistent with the present approach and the method is not applicable in these situations.

C. Assessing hidden compartments from epidemic surveillance data

Epidemiological surveillance provides the number of confirmed cases, deaths, date of first symptoms, or diagnosis; nothing with respect to the other compartments is commonly available. Actually, in the real scenario, the situation is much more complicated due to delays and other complex issues on surveillance counts [54, 55]. Using the case series $\mathcal{C}(t)$, we estimate infection rates λ_A and λ_I concomitantly with the initial conditions $(S^*, E^*, A^*, I^*, R^*)$ using the following calibration procedure:

- i. Select the time interval $[t_{cal}, t_{cal} + \Delta\tau]$ for which the reported case series $\mathcal{C}(t)$ will be analyzed. This time

window should be short enough to assume that infection rates λ_A and λ_I are approximately constant, but sufficiently large to have significant amount of data;

- ii. Using the time series of case and death counts, determine the probability p_I using Eq. (11) for a given ratio $r = p_A/p_I$, assumed to be a parameter of the method.
- iii. Consider an adiabatic approximation assuming that susceptible population varies much more slowly than the other compartments such that one can neglect its variation and take $S(t) \approx S^*$ as being constant over the investigated period.
- iv. Start with guessed initial values for the products $\gamma_A = \lambda_A S^*$ and $\gamma_I = \lambda_I S^*$ (to be fitted with data).
- v. Determine the number of undocumented cases N_R^* at $t = t_{\text{cal}}$ using the under-reporting coefficient calculated using Eqs. (5), (8), (11), and (13) and the number of confirmed cases $N_C^* = \mathcal{C}(t_{\text{cal}}) - \mathcal{C}(t_{\text{tr}})$ from case counting, where t_{tr} is a transient time to be chosen accordingly the epidemiological series. Remember that N_C^* encompasses all confirmed compartments; see Eq. (6).
- vi. Under these conditions the compartmental model provides a closed linear system $\dot{\mathbf{X}} = \mathbb{J}\mathbf{X}$ for the infectious compartments $\mathbf{X} = (E, A, I)$ where the Jacobian is given by

$$\mathbb{J} = \begin{bmatrix} -\mu_A & \gamma_A & \gamma_I \\ \mu_A & -(\beta_I + \beta_R + \beta_C) & 0 \\ 0 & \beta_I & -(\alpha_R + \alpha_C) \end{bmatrix}. \quad (14)$$

We assume that the solution is ruled by the leading term $\mathbf{X} \sim \mathbf{v}_1 \exp[\Lambda_1(t - t_{\text{cal}})]$ where $\mathbf{v}_1 = (v_E, v_A, v_I)$ is the principal eigenvector corresponding to the largest eigenvalue Λ_1 of \mathbb{J} , providing the following relations among initial conditions (E^*, A^*, I^*)

$$\frac{E^*}{A^*} \approx \frac{v_E}{v_A} \quad \text{and} \quad \frac{I^*}{A^*} \approx \frac{v_I}{v_A}. \quad (15)$$

Using again $\mathbf{X} \sim \mathbf{v}_1 \exp[\Lambda_1(t - t_{\text{cal}})]$, a closed system of initial conditions for (E^*, A^*, I^*) is obtained with the integration of Eq. (1f) to obtain

$$\Delta \mathcal{C} \approx (\beta_C A^* + \alpha_C I^*) \frac{e^{\Lambda_1 \Delta \tau} - 1}{\Lambda_1}, \quad (16)$$

where $\Delta \mathcal{C}$ is the increment of confirmed cases, available from data, during the interval $\Delta \tau$. If $\Lambda_1 \Delta \tau \ll 1$ we obtain

$$\beta_C A^* + \alpha_C I^* \approx \frac{\Delta \mathcal{C}}{\Delta \tau}. \quad (17)$$

Finally, the susceptible population is determined as

$$N_S^* = N - N_C^* - N_E^* - N_A^* - N_I^*, \quad (18)$$

implying that $S^* = N_S^*/N$, and the infection rates self-consistently estimated as $\lambda_A = \gamma_A/S^*$ and $\lambda_I = \gamma_I/S^*$.

- vii. Equations (1b) to (1f) are integrated in the interval $[t_{\text{cal}}, t_{\text{cal}} + \Delta \tau]$ and the dispersion with respect to the case counts is computed as

$$\Omega(\gamma_I, \gamma_A) = \int_{t_{\text{cal}}}^{t_{\text{cal}} + \Delta \tau} [\mathcal{C}(t) - C(t)]^2 dt. \quad (19)$$

- viii. The parameters γ_A and γ_I are incremented interactively and steps (iv) to (vii) are implemented using a bisection method to minimize $\Omega(\gamma_I, \gamma_A)$. In other words, a mesh with discrete values of (γ_I, γ_A) , with mesh space $(\Delta \gamma_I, \Delta \gamma_A)$, is varied searching for the minimal value of $\Omega(\gamma_I, \gamma_A)$. Then, the mesh space is reduced and the analysis repeated around the pair (γ_I, γ_A) that yielded the lowest Ω is the preceding step. This process is iterated 1000 times.

The choice of the transient time t_{tr} should compensate new epidemic factors such as new variants and waning immunity that lead to reinfections and new outbreaks. Another factor that can alter the susceptible population is the vaccination which also confers variable levels of immunity against infections. Vaccination also impacts both the IFR and CFR, such that the updated estimates of the IFR should be considered if the count series fueling the analysis is concomitant with vaccination, as the case of our current analysis; see Sec. III A.

III. RESULTS

A. Parameters and epidemic series

We applied the method to two types of count series available for Brazil, hereafter named Type-I and Type-II. The former consists of count series using release dates provided by epidemic surveillance departments of Brazilian federative units¹ which are aggregated and publicly available for all 5570 Brazillian municipalities [56]. These data do not yield the date of diagnosis and may present uncontrolled bias caused by reporting delays and should be used with care. The Type-II data sets contain dates of diagnosis and first symptoms onset. In this work, we use the publicly available Type-II data for Paraná (PR) [57] and Espírito Santo (ES) [58] states. The data are publicly available in the cited resources and the data aggregated for different municipalities, used in the present work, is available elsewhere [59]. A full description of these datasets can be found in the Supplementary Material (SM) [60].

We fixed the average values of the parameters $\mu_A^{-1} = 3.2$ d and $\beta_I^{-1} = 3.2$ d so that the mean incubation time is

¹ Brazil is divided into 26 states and 1 federal district. States aggregate municipalities with independent administrative structure. Cases are reported by municipalities to state's healthcare departments which release the information publicly.

of 6.4 d [6, 35]. The mean recovery time for symptomatic individuals was taken as $\alpha_R^{-1} = 3.2$ d [61]. Following [34, 35], asymptomatic cases were assumed to have the same recovering time such that $\beta_R^{-1} = \beta_I^{-1} + \alpha_R^{-1}$. Uncertainty analysis was done drawing μ_A , β_I , and α_R from Gamma distributions with standard deviation of 1.3 d, while an uniform distribution with 10% of uncertainty were used for calibrated γ_A and γ_I .

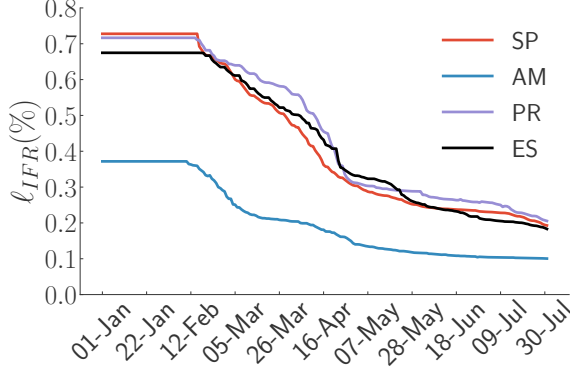


FIG. 2. Infection fatality ratio as a function of time, estimated for São Paulo (SP), Amazonas (AM), Paraná (PR), and Espírito Santo (ES) states considering their demographics and vaccination rates.

The IFR is the most critical parameter of our analysis. Since the time window we analyzed is concomitant with vaccination, a progressive reduction in the IFR is expected. To estimate the IFR reduction due to vaccines we proceeded as follows. The age-dependent IFR profile reported by Verdity [27], which yields an exponential increase with age and average IFR 0.68%, was considered. The number of persons who completed the vaccination (two or one shot depending on the vaccine type) as a function of time was extracted from surveillance systems, publicly available at Ref. [56]. Demographic data were obtained from *Instituto Brasileiro de Geografia e Estatística* (IBGE) [62]. Brazil followed a decreasing age prioritization strategy where elderly were vaccinated first down to the young population. We consider $g = 1, \dots, N_g$ group ages, in which $g = 1$ corresponds to ≥ 75 yr, $g = 2$ to 70 – 74 yr, \dots , $g = 16$ to 0 – 4 and assume that all vaccines shots were distributed according to this sequence. Using data for states, both vaccination rates and demographics [62], we calculated the average IFR as follows. Without vaccines, the average IFR is given by

$$\ell_{\text{IFR}} = \sum_{g=1}^{N_g} \ell_g n_g, \quad (20)$$

where ℓ_g and n_g are, respectively, the IFR and population fraction in the age group g . If x is the total fraction of the vaccinated population, the lower age group g^* who

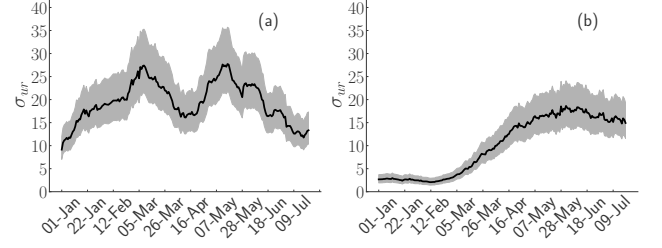


FIG. 3. Evolution of under-reporting coefficient σ_{ur} for the capital cities of (a) Manaus and (b) São Paulo estimated using moving time windows of three weeks for Type-I count series (see main text) as reported by state's surveillance departments [56]. The confidence interval of 95% is shown in the shaded region.

were vaccinated is given by

$$\sum_{g=1}^{g^*} f_g n_g < x < \sum_{g=1}^{g^*+1} f_g n_g, \quad (21)$$

where f_g is the fraction of the group age g who was vaccinated. Finally, if r_g is the IFR reduction of the vaccinated population of age group g , the corrected IFR becomes

$$\ell_{\text{IFR}} = \sum_{g=1}^{N_g} \ell_g n_g - \sum_{g=1}^{g^*} \ell_g n_g f_g (1 - r_g). \quad (22)$$

For sake of simplicity, we assumed that $f_g = f = 0.85$ and $r_g = r = 0.05$ uniform across all age groups. These parameters are consistent with typical protection rates associated to vaccines used in Brazil (Pfizer-Biotech, Sinovac and Astrazeneca). The IFR as a function of time for the four investigated states are presented in Fig. 2. The lower IFR for Amazonas's state reflects its young population (see SM [60]), while similar patterns are observed for the other analyzed states. Obviously, this is a simplified approach aiming at being qualitatively correct rather than quantitatively accurate. The used data is available in the SM [60].

B. Under-reporting coefficient

The evolution of σ_{ur} using Type-I count series of two capital cities of Brazil, which were severely impacted by COVID-19 second infection wave, namely Manaus and São Paulo [42], are presented in Fig. 3, for which the estimated delays between case and death confirmations were $t_{\text{delay}} = 7$ and 9 days, respectively; see Figs. S1(a) and (b) in the SM [60]. The delay is obtained by shifting the time series such that the peaks of deaths and cases coincide. We consider t_{tr} as January 1, 2021. Evolution patterns of σ_{ur} are different for these municipalities. While Manaus presents a high level of under-reporting (10 to 25) along the whole analyzed time series, in São

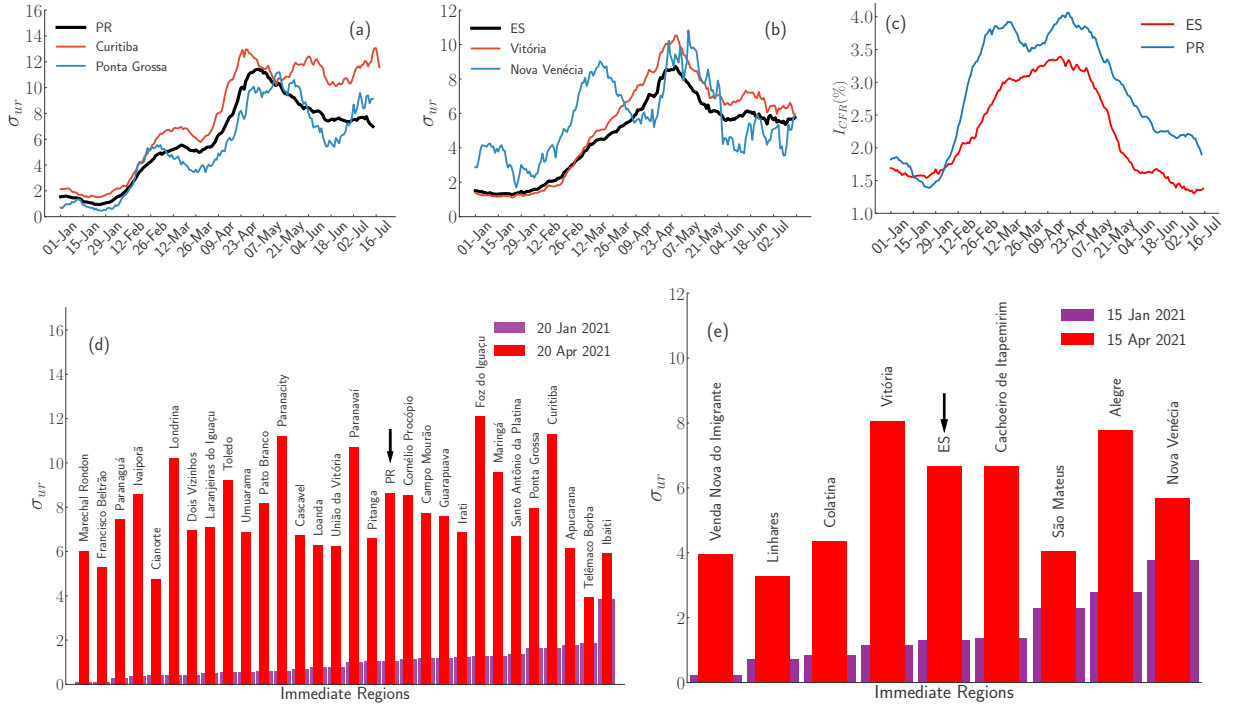


FIG. 4. Evolution of under-reporting coefficient for (a) PR and (b) ES states using time windows of three weeks. Two immediate regions of each state are presented in the corresponding panels. (c) Evolution of the CFR computed using delays $t_{\text{delay}} = 10$ d and 20 d for PR and ES states, respectively. Under-reporting coefficients for all immediate regions of (d) PR and (e) ES and the for states (indicated by arrows) computed when the CFR is low (January 2021) and high (April 2021).

Paulo, σ_{ur} increases from approximately 3 at the beginning of 2021 to 17 in June.

We analyzed Type-II count series for PR and ES states aggregating data of municipalities into immediate regions defined by IBGE [62] as a group of nearby municipalities of a same state with intense interchange for immediate needs (purchasing, work, healthcare, education, and so on). Case and death series for the PR state present a delay of $t_{\text{delay}} \approx 10$ d between death and positive test report. For ES state this delay is $t_{\text{delay}} \approx 20$ d.

The evolution of σ_{ur} computed with counts aggregated by states and two selected immediate regions are shown in Figures 4(a) and (b) for PR and ES, respectively. Curves for the 28 and 8 immediate regions of PR and ES, respectively, with the confidence intervals are available in Figs. S2 and S3 of the SM [60]. Note that CFR, Fig. 3(c), and σ_{ur} present different temporal patterns despite the correlation stated by Eq. (13). The second relevant outcome is the substantial variation of undocumented infection along the time and across different places with σ_{ur} varying approximately one order of magnitude in Figs. 4(a) and (b). The under-reporting coefficient for all immediate regions of both PR and ES states are presented in Figs. 4(d) and (e); the chosen dates correspond to low and high CFR in the respective state counts. The differences between immediate regions can differ largely in a same time window. The space-time variability reflects the high diversities of outbreak

across different places, due to unsynchronized and unequal responses to pandemics besides demographic, economic, and developmental heterogeneity of states as predicted [34] and later observed [42] for the first epidemic wave in Brazil.

C. Determination of the initial conditions

To apply the calibration method of Sec. II C, we performed the analysis for case counts of the PR state shown in Fig. 5; see Fig. S4 on SM [60] for the ES state. We further simplified the analysis assuming the same infection rate for both asymptomatic and symptomatic individuals prior diagnosis confirmation, $\lambda_A = \lambda_I$, implying in a single parameter to fit the data. The ratio between testing probabilities of symptomatic and asymptomatic individuals is fixed to $p_A/p_I = 0.1$. The calibrated curves match each other within the confidence intervals for a variation of one order of magnitude in this ratio. Typical calibration curves are presented in Fig. 5(a)-(i) for different times using a 14-day moving window of calibration. A forecast of one week is also presented to verify the calibration robustness, reproducing very well the short-term progression of the cumulative case count time series. The method also performs very well for smaller geographical scales such as immediate regions; see Fig. S5 of the SM [60].

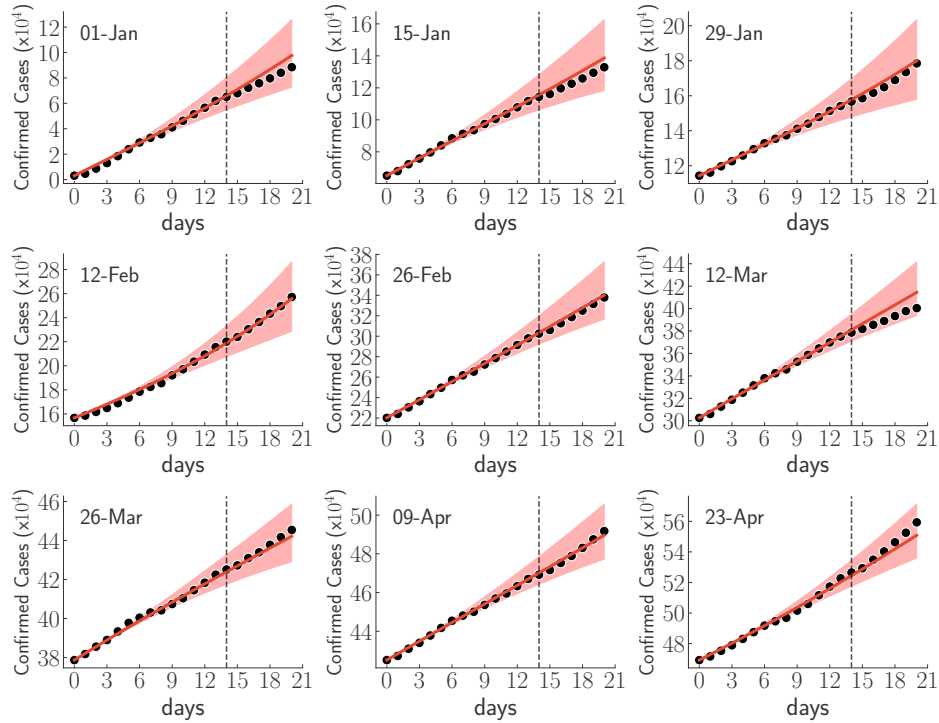


FIG. 5. Calibration curves for PR state in different time windows of 14 days indicated by the vertical lines. Initial day is indicated in the top of each panel. One week of forecasting is also shown. Symbols are the cumulative cases' counts while lines with shaded regions represent the calibrated curves and the corresponding confidence interval of 95%.

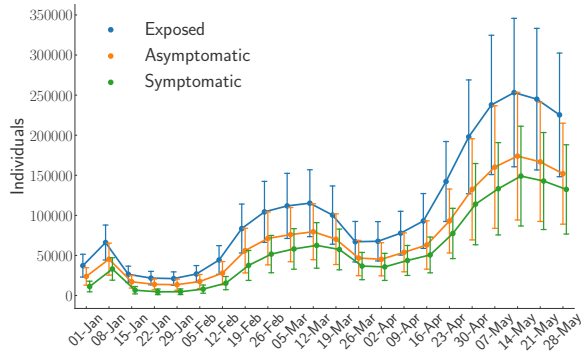


FIG. 6. Evolution of the undocumented compartments (exposed, asymptomatic and symptomatic) for the PR state since January 1, 2021.

The evolution of the undocumented epidemic compartments (exposed, asymptomatic, and symptomatic) yielded by the calibration method for PR state from January to May 2021 is presented in Fig. 6. Remark that the ratio between the total amount of infected individuals and the number of confirmed cases at a given day is much higher than the under-reporting coefficient shown in Fig. 4 since the latter refers to the final epidemic chain, where an infection ends documented or not, whereas the former refers to the amount of infected individuals in a given day which has not been documented yet. The peaks

of prevalence of infectious cases happen slightly before peaks of incidence of confirmed cases. Figure 6 shows an increase of the undocumented cases in the same period (middle April to May of 2022) when the under-reporting was higher for the PR state; Fig. 3(a). One explanation for this behavior is the vaccination which leads to less aggressive manifestation of the infections and lower seeking for medical attention and testing.

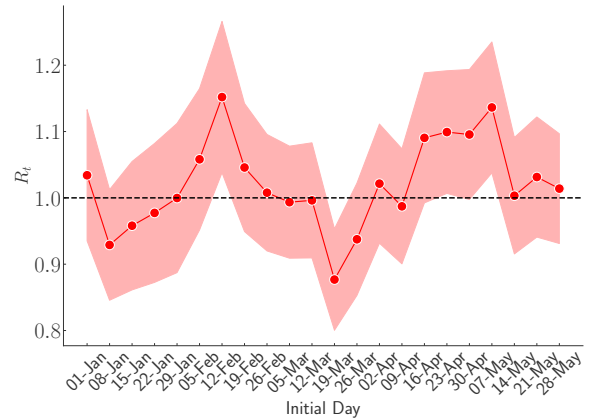


FIG. 7. Evolution of effective reproductive number R_t computed for the PR state considering $p_A/p_I = 0.1$ and $\lambda_A = \lambda_I$. The confidence interval of 95% is shown in the shaded region for the black curve.

The effective reproduction number for PR state is presented in Fig. 7. The calibration is sensitive to the variations and inflections in case count series, where the mean value of R_t oscillated between approximately 0.9 and 1.2. We performed a sensibility analysis of R_t and verified that its value is almost independent of the testing rates of asymptomatic compartments. More precisely, the curves of R_t collapses within the confidence interval when the ratios between testing probabilities p_A/p_I and infection rates λ_A/λ_I are varied by one order of magnitude.

IV. DISCUSSION

The pandemic caused by the SARS-CoV-2 led to unprecedented efforts gathering scientific community, epidemic surveillance, public authorities, and communication systems to provide almost real-time updated and publicly available counts for diagnosed infections, deaths, and other important statistics for COVID-19 spread across the globe. Available epidemic series, however, are still not ideal due to our limited capacity in documenting all infections in the due time. Moreover, these limitations vary enormously across different places and at different moments. However, this opens new avenues for construction and improvement of tools to extract information which are not explicit in data. A particularly promising strategy is the data-driven approach [34, 35, 38] where mathematical and mechanistic models are fueled by data, allowing to estimate variables which are not explicitly available. In the case of SARS-CoV-2 infections, the important class of asymptomatic or pre-symptomatic infections, in which individuals transmit the pathogen even without symptoms, are crucial being very costly to be detected in epidemic surveillance systems.

In the present work, we follow a data-driven approach using a compartmental model to estimate the amount of undocumented cases in the epidemic compartments which are not directly accessible in surveillance systems. The method allows to estimate the fraction of undocumented infections using case fatality ratio (CFR) and biological parameters that, in principle, can be estimated in controlled studies, in particular the infection fatality ratio (IFR). We applied the method to epidemic series of diagnosed cases and deaths of two Brazilian states where days of the symptoms onset were available. We selected the first semester of 2021 when Brazil was struck by a second epidemic wave of COVID-19, mainly driven the Gamma variant (lineage P.1). We calculated a under-reporting coefficient σ_{ur} , giving the ratio between infections which ends diagnosed or not. Our analysis reports a large variation of σ_{ur} along the time and also across different locations at a same period. The method allows to estimate the initial condition for the undocumented compartments, in particular the asymptomatic and exposed ones. While, on the one hand, the presented numbers

should be not interpreted as accurate estimates of actual epidemic prevalence, on the other hand, they clearly demonstrate that the infected individuals that can potentially seek for medical assistance are a minor part of all cases. Interestingly, the effective reproduction number is almost insensitive to the testing rate of asymptomatic cases, confirming that undocumented infections do not affect this important epidemic indicator.

The method can be generalized for stratified data including age contact matrices [63] or metapopulation approaches [34, 35]. However, the main lesson is that initial conditions for undocumented compartments can be inferred using a simple mechanistic approach, based on compartmental models fueled by epidemiological series of diagnosed death and cases. Nonetheless, the accuracy of methods depends on good estimates of biological parameters, mainly the IFR that changes as the epidemic scenario is altered. For example, vaccination is expected to reduce IFR while the emergence of more aggressive variants can increase it. We developed a simple data-driven approach to estimate the IFR evolution in terms of time series with vaccination rates. As a forthcoming continuation of the present work, we could investigate different time distributions for epidemic transitions, akin to applied epidemiology, using, for example, Monte Carlo approaches.

Code and data: Fortran and Python codes used for calibration and processing the epidemic series were made publicly in [59]. A description of the datasets and codes can be found in the SM [60].

Author contributions: **GSC:** Conceptualization; Formal analysis; Data curation; Investigation; Methodology; Software; Visualization; Writing - review & editing. **WC:** Conceptualization; Data curation; Methodology; Software; Validation; Visualization; Writing - review & editing. **SCF:** Conceptualization; Formal analysis; Funding acquisition; Methodology; Project administration; Writing - original draft.

Competing interests: Authors declare no competing interest.

ACKNOWLEDGMENTS

This work was partially supported by the Brazilian agencies *Coordenação de Aperfeiçoamento de Pessoal de Nível Superior* - CAPES (Grant no. 88887.507046/2020-00), *Conselho Nacional de Desenvolvimento Científico e Tecnológico* - CNPq (Grants no. 430768/2018-4 and 311183/2019-0) and *Fundação de Amparo à Pesquisa do Estado de Minas Gerais* - FAPEMIG (Grant no. APQ-02393-18). This study was financed in part by the *Coordenação de Aperfeiçoamento de Pessoal de Nível Superior* (CAPES) - Brasil - Finance Code 001.

- [1] J. T. Wu, K. Leung, and G. M. Leung, *Lancet* **395**, 689 (2020).
- [2] J. Zhang, M. Litvinova, Y. Liang, Y. Wang, W. Wang, S. Zhao, Q. Wu, S. Merler, C. Viboud, A. Vespignani, M. Ajelli, and H. Yu, *Science* **368**, 1481 (2020).
- [3] E. Estrada, *Phys. Rep.* **869**, 1 (2020).
- [4] M. Gilbert, G. Pullano, F. Pinotti, E. Valdano, C. Pioletto, P.-Y. Boëlle, E. D'Ortenzio, Y. Yazdanpanah, S. P. Eholie, M. Altmann, B. Gutierrez, M. U. G. Kraemer, and V. Colizza, *Lancet* **395**, 871 (2020).
- [5] R. Li, S. Pei, B. Chen, Y. Song, T. Zhang, W. Yang, and J. Shaman, *Science* **368**, 489 (2020).
- [6] Q. Li, X. Guan, P. Wu, X. Wang, L. Zhou, Y. Tong, R. Ren, K. S. Leung, E. H. Lau, J. Y. Wong, X. Xing, N. Xiang, Y. Wu, C. Li, Q. Chen, D. Li, T. Liu, J. Zhao, M. Liu, W. Tu, C. Chen, L. Jin, R. Yang, Q. Wang, S. Zhou, R. Wang, H. Liu, Y. Luo, Y. Liu, G. Shao, H. Li, Z. Tao, Y. Yang, Z. Deng, B. Liu, Z. Ma, Y. Zhang, G. Shi, T. T. Lam, J. T. Wu, G. F. Gao, B. J. Cowling, B. Yang, G. M. Leung, and Z. Feng, *N. Engl. J. Med.* **382**, 1199 (2020).
- [7] H. Nishiura, N. M. Linton, and A. R. Akhmetzhanov, *Int. J. Infect. Dis.* **93**, 284 (2020).
- [8] D. Baud, X. Qi, K. Nielsen-Saines, D. Musso, L. Pomar, and G. Favre, *Lancet Infect. Dis.* **20**, 773 (2020).
- [9] X. He, E. H. Y. Lau, P. Wu, X. Deng, J. Wang, X. Hao, Y. C. Lau, J. Y. Wong, Y. Guan, X. Tan, X. Mo, Y. Chen, B. Liao, W. Chen, F. Hu, Q. Zhang, M. Zhong, Y. Wu, L. Zhao, F. Zhang, B. J. Cowling, F. Li, and G. M. Leung, *Nat. Med.* **26**, 672 (2020).
- [10] L. C. Tindale, J. E. Stockdale, M. Coombe, E. S. Garlock, W. Y. V. Lau, M. Saraswat, L. Zhang, D. Chen, J. Wallinga, and C. Colijn, *eLife* **9**, 2020.03.03.20029983 (2020).
- [11] J. C. Emery, T. W. Russell, Y. Liu, J. Hellewell, C. A. Pearson, K. E. Atkins, P. Klepac, A. Endo, C. I. Jarvis, N. G. Davies, E. M. Rees, S. R. Meakin, A. Rosello, K. van Zandvoort, J. D. Munday, W. J. Edmunds, T. Jombart, M. Auzenberg, E. S. Nightingale, M. Jit, S. Abbott, D. Simons, N. I. Bosse, Q. J. Leclerc, S. R. Procter, C. J. Villabona-Arenas, D. C. Tully, A. K. Deol, F. Y. Sun, S. Hué, A. M. Foss, K. Prem, G. Medley, A. Gimma, R. Lowe, S. Clifford, M. Quaife, C. Diamond, H. P. Gibbs, B. J. Quilty, K. O'Reilly, G. M. Knight, R. M. Eggo, A. J. Kucharski, S. Funk, S. Flasche, and R. M. Houben, *eLife* **9**, 1 (2020).
- [12] N. G. Davies, P. Klepac, Y. Liu, K. Prem, M. Jit, and R. M. Eggo, *Nat. Med.* **26**, 1205 (2020).
- [13] M. Lipsitch and N. E. Dean, *Science* **370**, 763 (2020).
- [14] N. G. Davies, S. Abbott, R. C. Barnard, C. I. Jarvis, A. J. Kucharski, J. D. Munday, C. A. B. Pearson, T. W. Russell, D. C. Tully, A. D. Washburne, T. Wenseleers, A. Gimma, W. Waites, K. L. M. Wong, K. van Zandvoort, J. D. Silverman, K. Diaz-Ordaz, R. Keogh, R. M. Eggo, S. Funk, M. Jit, K. E. Atkins, and W. J. Edmunds, *Science* **372**, eabg3055 (2021).
- [15] L. F. Buss, C. A. Prete, C. M. M. Abraham, A. Mendrone, T. Salomon, C. de Almeida-Neto, R. F. O. França, M. C. Belotti, M. P. S. S. Carvalho, A. G. Costa, M. A. E. Crispim, S. C. Ferreira, N. A. Fraiji, S. Gurzenda, C. Whittaker, L. T. Kamaura, P. L. Takecian, P. da Silva Peixoto, M. K. Oikawa, A. S. Nishiya, V. Rocha, N. A. Salles, A. A. de Souza Santos, M. A. da Silva, B. Custer, K. V. Parag, M. Barral-Netto, M. U. G. Kraemer, R. H. M. Pereira, O. G. Pybus, M. P. Busch, M. C. Castro, C. Dye, V. H. Nascimento, N. R. Faria, and E. C. Sabino, *Science* **371**, 288 (2020).
- [16] D. Sridhar and D. Gurdasani, *Science* **371**, 230 (2021).
- [17] A. Pan, L. Liu, C. Wang, H. Guo, X. Hao, Q. Wang, J. Huang, N. He, H. Yu, X. Lin, S. Wei, and T. Wu, *JAMA* **323**, 1915 (2020).
- [18] S. T. Ali, L. Wang, E. H. Y. Lau, X.-K. Xu, Z. Du, Y. Wu, G. M. Leung, and B. J. Cowling, *Science* **369**, 1106 (2020).
- [19] A. Goyal, D. B. Reeves, E. F. Cardozo-Ojeda, J. T. Schiffer, and B. T. Mayer, *eLife* **10** (2021), 10.7554/elife.63537.
- [20] S. Flaxman, S. Mishra, A. Gandy, H. J. T. Unwin, T. A. Mellan, H. Coupland, C. Whittaker, H. Zhu, T. Berah, J. W. Eaton, M. Monod, P. N. Perez-Guzman, N. Schmit, L. Cilloni, K. E. C. Ainslie, M. Baguelin, A. Boonyasiri, O. Boyd, L. Cattarino, L. V. Cooper, Z. Cucunubá, G. Cuomo-Dannenburg, A. Dighe, B. Djaafara, I. Dorigatti, S. L. van Elsland, R. G. FitzJohn, K. A. M. Gaythorpe, L. Geidelberg, N. C. Grassly, W. D. Green, T. Hallett, A. Hamlet, W. Hinsley, B. Jeffrey, E. Knock, D. J. Laydon, G. Nedjati-Gilani, P. Nouvellet, K. V. Parag, I. Siveroni, H. A. Thompson, R. Verity, E. Volz, C. E. Walters, H. Wang, Y. Wang, O. J. Watson, P. Winskill, X. Xi, P. G. T. Walker, A. C. Ghani, C. A. Donnelly, S. Riley, M. A. C. Vollmer, N. M. Ferguson, L. C. Okell, and S. Bhatt, *Nature* **584**, 257 (2020).
- [21] A. Cori, N. M. Ferguson, C. Fraser, and S. Cauchemez, *Am. J. Epidemiol.* **178**, 1505 (2013).
- [22] K. M. Gostic, L. McGough, E. B. Baskerville, S. Abbott, K. Joshi, C. Tedijanto, R. Kahn, R. Niehus, J. A. Hay, P. M. De Salazar, J. Hellewell, S. Meakin, J. D. Munday, N. I. Bosse, K. Sherratt, R. N. Thompson, L. F. White, J. S. Huisman, J. Scire, S. Bonhoeffer, T. Stadler, J. Wallinga, S. Funk, M. Lipsitch, and S. Cobey, *PLOS Comput. Biol.* **16**, e1008409 (2020).
- [23] K. Mizumoto, K. Kagaya, A. Zarebski, and G. Chowell, *Eurosurveillance* **25** (2020), 10.2807/1560-7917.ES.2020.25.10.2000180.
- [24] O. Byambasuren, M. Cardona, K. Bell, J. Clark, M.-L. McLaws, and P. Glasziou, *Off. J. Assoc. Med. Microbiol. Infect. Dis. Canada* **5**, 223 (2020).
- [25] D. Buitrago-Garcia, D. Egli-Gany, M. J. Counotte, S. Hossmann, H. Imeri, A. M. Ipekci, G. Salanti, and N. Low, *PLoS Med.* **17**, 1 (2020).
- [26] J. P. A. Ioannidis, *Bull. World Health Organ.* **99**, 19 (2021).
- [27] R. Verity, L. C. Okell, I. Dorigatti, P. Winskill, C. Whittaker, N. Imai, G. Cuomo-Dannenburg, H. Thompson, P. G. Walker, H. Fu, A. Dighe, J. T. Griffin, M. Baguelin, S. Bhatia, A. Boonyasiri, A. Cori, Z. Cucunubá, R. FitzJohn, K. Gaythorpe, W. Green, A. Hamlet, W. Hinsley, D. Laydon, G. Nedjati-Gilani, S. Riley, S. van Elsland, E. Volz, H. Wang, Y. Wang, X. Xi, C. A. Donnelly, A. C. Ghani, and N. M. Ferguson, *Lancet Infect. Dis.* **20**, 669 (2020).
- [28] C. M. Romano, A. C. Felix, A. V. de Paula, J. G.

- de Jesus, P. S. Andrade, D. Cândido, F. M. de Oliveira, A. C. Ribeiro, F. C. da Silva, M. Inemami, A. A. Costa, C. O. D. Leal, W. M. Figueiredo, C. S. Pannuti, W. M. de Souza, N. R. Faria, and E. C. Sabino, *Rev. Inst. Med. Trop. Sao Paulo* **63**, 0 (2021).
- [29] G. Pullano, L. Di Domenico, C. E. Sabbatini, E. Valdano, C. Turbelin, M. Debin, C. Guerrisi, C. Kengne-Kuetche, C. Souty, T. Hanslik, T. Blanchon, P.-Y. Boëlle, J. Figoni, S. Vaux, C. Campese, S. Bernard-Stoecklin, and V. Colizza, *Nature* **590**, 134 (2021).
- [30] F. S. Lu, A. T. Nguyen, N. B. Link, M. Molina, J. T. Davis, M. Chinazzi, X. Xiong, A. Vespignani, M. Lipsitch, and M. Santillana, *PLOS Comput. Biol.* **17**, e1008994 (2021).
- [31] R. Subramanian, Q. He, and M. Pascual, *Proc. Natl. Acad. Sci.* **118**, e2019716118 (2021).
- [32] N. J. Irons and A. E. Raftery, *Proc. Natl. Acad. Sci. U. S. A.* **118** (2021), 10.1073/pnas.2103272118.
- [33] P. C. Hallal, F. P. Hartwig, B. L. Horta, M. F. Silveira, C. J. Struchiner, L. P. VIDALETTI, N. A. Neumann, L. C. Pellanda, O. A. Dellagostin, M. N. Burattini, G. D. Victora, A. M. B. Menezes, F. C. Barros, A. J. D. Barros, and C. G. Victora, *Lancet Glob. Heal.* **8**, e1390 (2020).
- [34] G. S. Costa, W. Cota, and S. C. Ferreira, *Phys. Rev. Res.* **2**, 043306 (2020), 2011.03380.
- [35] A. Arenas, W. Cota, J. Gómez-Gardeñes, S. Gómez, C. Granell, J. T. Matamalas, D. Soriano-Paños, and B. Steinegger, *Phys. Rev. X* **10**, 041055 (2020).
- [36] P. Ashcroft, S. Lehtinen, D. C. Angst, N. Low, and S. Bonhoeffer, *eLife* **10**, 1 (2021).
- [37] L. Ferretti, C. Wymant, M. Kendall, L. Zhao, A. Nurtay, L. Abeler-Dörner, M. Parker, D. Bonsall, and C. Fraser, *Science* **368**, eabb6936 (2020).
- [38] A. Aleta and Y. Moreno, *BMC Med.* **18**, 157 (2020).
- [39] A. Aleta, D. Martín-Corral, A. Pastore y Piontti, M. Ajelli, M. Litvinova, M. Chinazzi, N. E. Dean, M. E. Halloran, I. M. Longini Jr, S. Merler, A. Pentland, A. Vespignani, E. Moro, and Y. Moreno, *Nat. Hum. Behav.* **4**, 964 (2020).
- [40] J. Dehning, J. Zierenberg, F. P. Spitzner, M. Wibral, J. P. Neto, M. Wilczek, and V. Priesemann, *Science* **369**, eabb9789 (2020).
- [41] B. F. Maier and D. Brockmann, *Science* **368**, 742 (2020).
- [42] M. C. Castro, S. Kim, L. Barberia, A. F. Ribeiro, S. Gurzenda, K. B. Ribeiro, E. Abbott, J. Blossom, B. Rache, and B. H. Singer, *Science* **372**, 821 (2021).
- [43] M. Keeling and P. Rohani, *Modeling Infectious Diseases in Humans and Animals* (Princeton University Press, 2008).
- [44] N. M. Ferguson, D. Laydon, G. Nedjati-Gilani, N. Imai, K. Ainslie, M. Baguelin, S. Bhatia, A. Boonyasiri, Z. Cucunubá, G. Cuomo-Dannenburg, A. Dighe, I. Dorigatti, H. Fu, K. Gaythorpe, W. Green, A. Hamlet, W. Hinsley, L. C. Okell, S. Van Elsland, H. Thompson, R. Verity, E. Volz, H. Wang, Y. Wang, P. Gt Walker, C. Walters, P. Winskill, C. Whittaker, C. A. Donnelly, S. Riley, and A. C. Ghani, *Report 9: Impact of non-pharmaceutical interventions (NPIs) to reduce COVID19 mortality and healthcare demand*, Tech. Rep. March (2020).
- [45] E. C. Sabino, L. F. Buss, M. P. S. Carvalho, C. A. Prete, M. A. E. Crispim, N. A. Fraiji, R. H. M. Pereira, K. V. Parag, P. da Silva Peixoto, M. U. G. Kraemer, M. K. Oikawa, T. Salomon, Z. M. Cucunuba, M. C. Castro, A. A. de Souza Santos, V. H. Nascimento, H. S. Pereira, N. M. Ferguson, O. G. Pybus, A. Kucharski, M. P. Busch, C. Dye, and N. R. Faria, *The Lancet* **397**, 452 (2021).
- [46] A. Vazquez, *Phys. Rev. E* **103**, 042306 (2021).
- [47] S. A. Lauer, K. H. Grantz, Q. Bi, F. K. Jones, Q. Zheng, H. R. Meredith, A. S. Azman, N. G. Reich, and J. Lessler, *Ann. Intern. Med.* **172**, 577 (2020).
- [48] D. S. Candido, I. M. Claro, J. G. de Jesus, W. M. Souza, F. R. R. Moreira, S. Dellicour, T. A. Mellan, L. du Plessis, R. H. M. Pereira, F. C. S. Sales, E. R. Manuli, J. Théze, L. Almeida, M. T. Menezes, C. M. Voloch, M. J. Fumagalli, T. M. Coletti, C. A. M. da Silva, M. S. Ramundo, M. R. Amorim, H. H. Hoeltgebaum, S. Mishra, M. S. Gill, L. M. Carvalho, L. F. Buss, C. A. Prete, J. Ashworth, H. I. Nakaya, P. S. Peixoto, O. J. Brady, S. M. Nicholls, A. Tanuri, Á. D. Rossi, C. K. V. Braga, A. L. Gerber, A. P. de C. Guimarães, N. Gaburo, C. S. Alencar, A. C. S. Ferreira, C. X. Lima, J. E. Levi, C. Granato, G. M. Ferreira, R. S. Francisco, F. Granja, M. T. Garcia, M. L. Moretti, M. W. Perroud, T. M. P. P. Castiñeiras, C. S. Lazari, S. C. Hill, A. A. de Souza Santos, C. L. Simeoni, J. Forato, A. C. Sposito, A. Z. Schreiber, M. N. N. Santos, C. Z. de Sá, R. P. Souza, L. C. Resende-Moreira, M. M. Teixeira, J. Hubner, P. A. F. Leme, R. G. Moreira, M. L. Nogueira, N. M. Ferguson, S. F. Costa, J. L. Proenca-Modena, A. T. R. Vasconcelos, S. Bhatt, P. Lemey, C.-H. Wu, A. Rambaut, N. J. Loman, R. S. Aguiar, O. G. Pybus, E. C. Sabino, and N. R. F. and, *Science* **369**, 1255 (2020).
- [49] S. Moore, E. M. Hill, M. J. Tildesley, L. Dyson, and M. J. Keeling, *Lancet Infect. Dis.* **21**, 793 (2021).
- [50] L. Di Domenico, G. Pullano, C. E. Sabbatini, P.-Y. Boëlle, and V. Colizza, *BMC Med.* **18**, 240 (2020).
- [51] K. Kupferschmidt and M. Wadman, *Science* **372**, 1375 (2021).
- [52] F. Ahmed, N. Ahmed, C. Pissarides, and J. Stiglitz, *Lancet Public Heal.* **5**, e240 (2020).
- [53] K. Sun, W. Wang, L. Gao, Y. Wang, K. Luo, L. Ren, Z. Zhan, X. Chen, S. Zhao, Y. Huang, Q. Sun, Z. Liu, M. Litvinova, A. Vespignani, M. Ajelli, C. Viboud, and H. Yu, *Science* **371**, eabe2424 (2021).
- [54] L. S. Bastos, T. Economou, M. F. C. Gomes, D. A. M. Villela, F. C. Coelho, O. G. Cruz, O. Stoner, T. Bailey, and C. T. Codeço, *Stat. Med.* **38**, 4363 (2019).
- [55] L. S. Bastos, R. P. Niquini, R. M. Lana, D. A. M. Villela, O. G. Cruz, F. C. Coelho, C. T. Codeço, and M. F. C. Gomes, *Cad. Saude Publica* **36** (2020), 10.1590/0102-311x00070120.
- [56] W. Cota, *SciELOPreprints*.362 (2020), 10.1590/SciELOPreprints.362.
- [57] G. do Estado do Paraná, (2021), Boletim - Informe Epidemiológico Coronavírus (COVID-19), <https://www.saude.pr.gov.br/Pagina/Coronavirus-COVID-19> [Online; accessed 08-Sep-2021].
- [58] G. do Estado do Espírito Santo, (2021), COVID-19 - Painel COVID-19 - Estado do Espírito Santo, <https://coronavirus.es.gov.br/painel-covid-19-es> [Online; accessed 08-Sep-2021].
- [59] “Codes and datasets are freely available at <https://github.com/ghscosta/covid19-cal>.”.
- [60] “Supplementary material.”.
- [61] J. M. Read, J. R. E. Bridgen, D. A. T. Cummings, A. Ho, and C. P. Jewell, *Philos. Trans. R. Soc. B Biol. Sci.* **376**, 20200265 (2021).
- [62] Instituto Brasileiro de Geografia e Estatística (IBGE),

Divisão Regional do Brasil em Regiões Geográficas Imediatas e Regiões Geográficas Intermediárias (Instituto Brasileiro de Geografia e Estatística Rio de Janeiro, 2017).

[63] K. Prem, A. R. Cook, and M. Jit, [PLOS Comput. Biol.](#) **13**, e1005697 (2017).